Mechanism-Based Inhibitors of CD38: A Mammalian Cyclic ADP-Ribose Synthetase†

Anthony A. Sauve and Vern L. Schramm*

Department of Biochemistry, Albert Einstein College of Medicine, 1300 Morris Park Avenue, Bronx, New York 10461

Received March 27, 2002

ABSTRACT: The soluble domain of human CD38 catalyzes the conversion of NAD^+ to cyclic ADP-ribose and to ADP-ribose via a common covalent intermediate [Sauve, A. A., Deng, H. T., Angelletti, R. H., and Schramm, V. L. (2000) *J. Am. Chem. Soc. 122*, 7855−7859]. Here we establish that mechanism-based inhibitors can be produced by chemical stabilization of this intermediate. The compounds nicotinamide 2′-deoxyriboside (**1**), 5-methylnicotinamide 2′-deoxyriboside (**2**), and pyridyl 2′-deoxyriboside (**3**) were synthesized and evaluated as inhibitors for human CD38. The nicotinamide derivatives **1** and **2** were inhibitors of the enzyme as determined by competitive behavior in CD38-catalyzed conversion of nicotinamide guanine dinucleotide (NGD^+) to cyclic GDP-ribose. The K_i values for competitive inhibition were 1.2 and 4.0 μM for **1** and **2**, respectively. Slow-onset characteristics of reaction progress curves indicated a second higher affinity state of these two inhibitors. Inhibitor off-rates were slow with rate constants k_{off} of 1.5×10^{-5} s^{-1} for **1** and 2.5×10^{-5} s^{-1} for **2**. Apparent dissociation constants $K_{i(total)}$ for **1** and **2** were calculated to be 4.5 and 12.5 nM, respectively. The similar values for k_{off} are consistent with the hydrolysis of common enzymatic intermediates formed by the reaction of **1** and **2** with the enzyme. Both form covalently attached deoxyribose groups to the catalytic site nucleophile. Chemical evidence for this intermediate is the ability of nicotinamide to rescue enzyme activity after inactivation by either **1** or **2**. A covalent intermediate is also indicated by the ability of CD38 to catalyze base exchange, as observed by conversion of **2** to **1** in the presence of nicotinamide. The deoxynucleosides **1** and **2** demonstrate that the chemical determinants for mechanism-based inhibition of CD38 can be satisfied by nucleosides that lack the 5′-phosphate, the adenylate group, and the 2′-hydroxyl moiety. In addition, these compounds reveal the mechanism of CD38 catalysis to proceed by the formation of a covalent intermediate during normal catalytic turnover with faster substrates. The covalent 2′-deoxynucleoside inactivators of CD38 are powerful inhibitors by acting as good substrates for formation of the covalent intermediate but are poor leaving groups from the intermediate complex because hydrolytic assistance of the 2′-hydroxyl group is lacking. The removal of the adenylate nucleophile required for the cyclization reaction provides slow hydrolysis as the only exit from the covalent complex.

CD38[1] is a membrane-anchored homodimeric ectoenzyme common to a variety of immune cells (*1*) and other tissues (*2*) including pancreas (*3*), kidney (*4*), and brain (*5*). CD38 is homologous to BST-1 (*6*, *7*), bone stromal cell antigen, and invertebrate ADP-ribosyl cyclases (*8*, *9*) and catalyzes the formation of cyclic ADP-ribose (cADPR, *10*) from NAD^+ (Scheme 1; *11*, *12*). cADPR is a potent second messenger that directly activates Ca^{2+} release inside of cells via an IP_3-independent mechanism (*13*−*15*) thought to be mediated by ryanodine receptors (*13*). Recent evidence suggests that cADPR and CD38 may play a crucial role in the human immune response by activation of the cell-mediated neutrophil response to bacterial infection (*16*) and associated inflammatory physiology (*16*, *17*). ADP-ribosyl cyclase and cADPR signaling has also been demonstrated in plants as mediator of the absciscic acid activated stress response (*18*). Not surprisingly, the ADP-ribosyl cyclases have been targets for inhibitor design (*19*−*23*). Also, analogues of cADPR with antagonistic (*24*−*27*) or agonistic (*28*−*34*) properties have been reported. Most of the inhibitors and cADPR analogues are phosphorylated compounds (*13*) and have practical limitations affecting their use in whole cell or whole tissue investigations because of the difficulty of passing charges across cell membranes (*13*). Although altered inhibitor structure to nucleosides could potentially make compounds more cell permeant, no reports of nucleoside-based CD38 or ADP-ribosyl cyclase inhibitors have appeared.

In prior work, the mononucleotide *ara*-F-NMN^+ was shown to be a potent inhibitor of CD38 with a K_i value of 61 nM (*23*). This inhibitor was the most powerful reported for CD38 and was similar to the value (169 nM; *20*) reported for the dinucleotide inhibitor *ara*-F-NAD^+ (*19*). To assess the effects of further truncations in the structure of *ara*-F-NMN^+, 2′-deoxynucleoside derivatives devoid of both the

† This research was supported by NIH Grant AI34342 to V.L.S.

* To whom correspondence should be addressed. Telephone: (718) 430-2813. Fax: (718) 430-8565. E-mail: vern@aecom.yu.edu.

[1] Abbreviations: CD38, cell developmental protein 38; NGD^+, nicotinamide guanine dinucleotide; cADPR, cyclic ADP-ribose; cGDPR, cyclic GDP-ribose; *ara*-F-NMN^+, arabinosyl-2′-fluoro-2′-deoxynicotinamide mononucleotide; NMN^+, nicotinamide mononucleotide.

10.1021/bi0258795 CCC: $22.00
Published on Web 06/07/2002

Scheme 1: NAD^+ Cyclization Reaction Catalyzed by ADP-ribosyl Cyclases

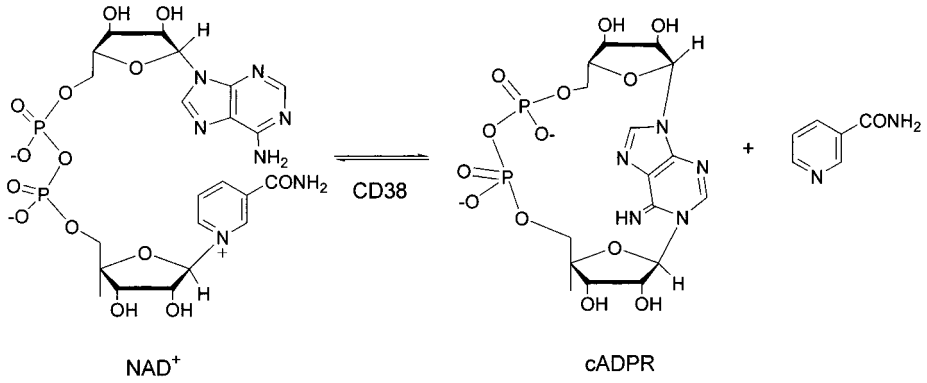

fluorine atom at the 2′-position and the phosphate group at the 5′-position were synthesized. These compounds bind to CD38 with dissociation constants in the low micromolar range and react subsequently to inactivate CD38 via a covalent mechanism, resulting in overall inhibition constants as low as 4.5 nM. These relatively simple structures are the first nucleosides shown to potently inhibit an ADP-ribosyl cyclase. In consequence of deoxynucleoside structures, they are expected to have better membrane permeability than their phosphorylated counterparts. They may find use in whole cell and whole tissue investigations of CD38 and cADPR action. The synthesis and characterization of these compounds as inhibitors of human CD38 are presented.

MATERIALS AND METHODS

Reagents for chemical synthesis were obtained from commercial vendors and were used as received. The synthesis of 1-α-chloro-3,5-di-*O*-*p*-chlorobenzoyl-2-deoxyribofuranose (**4**) was synthesized as reported (*41*). This sugar could be stored with a P_2O_5 sidearm for desiccation at −78 °C. [2′-^{3}H]Deoxyuridine was obtained from ARC in 5 mCi quantity and used as received. Thymidine phosphorylase and alkaline phosphatase was obtained from Sigma. NMR data were obtained on a Bruker DRX-300 instrument.

Synthesis of β-3′,5′-Di-O-p-chlorobenzoyl-1′-nicotinamide 2′-Deoxyriboside. Compound **4** (100 mg, 0.3 mmol) was added to a flame-dried flask containing 90 mg (0.8 mmol) of nicotinamide. To a second flask the additions were 20 mg (0.2 mmol) of nicotinamide, 100 mg of $AgSbF_6$ (0.3 mmol), and 5 mL of acetonitrile added to dissolve the salt. The silver solution was cooled to 0 °C with ice and then added rapidly by syringe to the flask containing the base and sugar. The solution was stirred while chilled in an ice bath, and a grayish precipitate formed. The reaction was stirred for 2 h, chilled, then warmed to room temperature, and stirred an additional 2 h. The reaction mixture was evaporated, and the residue was redissolved in MeOH and filtered through Celite. The filtrate was evaporated. The material was determined by NMR to contain the desired product in a mixture of stereoisomers (9:1 β:α) in a yield of 85%. ^{1}H NMR (MeOD-d_3): δ 9.54 (s, 1H), 9.25 (s, 1H), 8.93 (d, 1H), 8.2 (m, 1H), 8.0−7.8 (m, 4H), 7.6−7.3 (m, 4H), 6.79 (t, 1H), 5.77 (m, 1H), 5.01 (m, 1H), 4.99−4.4 (m, 3H), 3.44 (m, 1H), 2.9 (m, 1H).

*Synthesis of β-Nicotinamide 2′-Deoxyriboside (**1**).*[2] The above material was subjected to deprotection without further purification by treatment with 5 mL of 2 M NH_3 in MeOH at −20 °C. This solution was reacted for 8 h at −20 °C. TLC was used to monitor the reaction. The MeOH and NH_3 were evaporated at reduced pressure, and the residue was redissolved in 300 μL of methanol. Water (1 mL) was then added. A gummy precipitate was removed by centrifugation, and the aqueous phase was purified by HPLC to yield pure α and β deprotected isomers of **1**. These isomers were analyzed by ^{1}H NMR. Inhibitor solutions were measured at 266 nm for absorbance (concentration) and frozen upon isolation by HPLC and placed at −78 °C for later use. ^{1}H NMR (D_2O): δ 9.5 (s, 1H), 9.18 (d, 1H), 8.84 (d, 1H), 8.16 (t, 1H), 6.56 (t, 1H), 4.47 (m, 1H), 4.29 (m, 1H), 4.5−4.0 (m, 2H), 3.0 (m, 1H), 2.82 (m, 1H). MS: $M^+ = 239$.

Synthesis of β-3′,5′-Di-O-p-chlorobenzoyl-1′-(5-methylnicotinamide) 2′-Deoxyriboside. Compound **4** (100 mg, 0.3 mmol) was added to a flask along with 50 mg (0.4 mmol) of 5-methylnicotinamide. To this flask was added 2 mL of CH_2Cl_2, and the flask was kept on ice. To a second flask was added 50 mg (0.4 mmol) of 5-methylnicotinamide, and 2 mL of acetonitrile was added. The solution was heated to 50 °C to dissolve the 5-methylnicotinamide and subsequently cooled to room temperature. $AgSbF_6$ (100 mg, 0.3 mmol) was added, and the silver solution was cooled to 0 °C with an ice bath. After several minutes on ice the contents of the silver solution were rapidly transferred by syringe to the flask containing the base and sugar. The solution was stirred while chilled by an ice bath, and a grayish precipitate formed. The reaction was stirred for 2 h, chilled, then warmed to room temperature, and stirred an additional 2 h. The reaction mixture was evaporated, and the residue was redissolved in MeOH and filtered through Celite. The filtrate was then evaporated. The material was determined by NMR to be a mixture of stereoisomers in a ratio of 4.2:1 (β:α) in a yield of 95%. ^{1}H NMR (CD_3CN): δ 9.298 (s, 1H), 9.017 (s, 1H), 8.804 (s, 1H), 8.275 (d, 2H), 8.04 (d, 2H), 7.77 (d, 2H), 7.64 (d, 2H), 6.78 (t, 1H), 5.90 (m, 1H), 5.178 (m, 1H), 4.99−4.7 (m, 2H), 3.44 (m, 1H), 3.1 (m, 1H), 2.66 (s, 3H).

*Synthesis of β-5-Methylnicotinamide 2′-Deoxyriboside (**2**).* This material was subjected to deprotection without further purification by addition of 4 mL of 2 M NH_3 in MeOH added at −20 °C, and the reaction was permitted to go for 8 h at

[2] The synthesis of this compound by a different route has been reported previously without data to characterize the product (*42*).

−20 °C. The MeOH and NH_3 were then evaporated at reduced pressure, and the residue was redissolved in 1 mL of cold water. After trituration with water the suspension was spun to remove precipitate, and the aqueous phase was purified by HPLC to yield the pure α and β deprotected isomers of **2**. These isomers could be analyzed by ^{1}H NMR by rapid evaporation and redissolution in D_2O. Inhibitor solutions were measured at 273 nm for absorbance (concentration) and frozen upon isolation by HPLC and placed at −78 °C. ^{1}H NMR (D_2O): δ 9.73 (s, 1H), 9.43 (s, 1H), 9.11 (s, 1H), 6.86 (t, 2H), 4.64 (m, 1H), 4.11 (m, 1H), 4.04−3.78 (m, 3H), 3.17 (m, 1H), 2.96 (s, 3H), 2.84 (m, 1H).

Synthesis of β-3′,5′-Di-O-p-chlorobenzoyl-1′-pyridyl 2′-Deoxyriboside. Compound **4** (50 mg, 0.15 mmol) was added to a flask. Additions to a second flask were 30 μL of pyridine, 50 mg of $AgSbF_6$ (0.15 mmol), and 5 mL of acetonitrile/CH_2Cl_2 (1:4) to dissolve the salt. The silver solution was cooled to 0 °C with ice and then added to the flask containing the sugar. The solution was stirred while chilled by ice bath, and a precipitate was observed to form. The reaction was stirred for 2 h, chilled, and then warmed to room temperature overnight. The reaction mixture was evaporated, and the residue was redissolved in MeOH and filtered through Celite. The filtrate was then evaporated. The material was determined by NMR to be a mixture of stereoisomers (14.3:1, β:α) in a yield of 95%. ^{1}H NMR (CD_3CN): δ 9.19 (d, 2H), 8.72 (t, 1H), 8.27 (t, 2H), 8.0−7.8 (m, 4H), 7.7−7.5 (m, 4H), 6.88 (t, 1H), 5.92 (m, 1H), 6.78 (t, 1H), 5.2 (m, 1H), 4.9 (m, 1H), 3.4 (m, 1H), 3.0 (m, 1H).

*Synthesis of β-Pyridyl 2′-Deoxyriboside (**3**).* The protected material above was subjected to deprotection without further purification by addition of 4 mL of 2 M NH_3 in MeOH added at 0 °C, and the reaction was permitted to go for 12 h at 4 °C. At the end of this time TLC indicated total consumption of starting material. The MeOH and NH_3 were then evaporated at reduced pressure, and the residue was redissolved in 300 μL of methanol followed by addition of 1 mL of water. After trituration with water the suspension was spun to remove precipitate, and the aqueous phase was purified by HPLC to yield the pure α and β deprotected isomers in a ratio of 10.4:1 (β:α). ^{1}H NMR (D_2O): δ 9.17 (d, 2H), 8.72 (t, 1H), 8.24 (t, 2H), 6.66 (t, 2H), 4.64 (m, 1H), 4.44 (dd, 1H), 4.04 (dd, 1H), 3.92 (dd, 1H), 2.99 (m, 1H), 2.74 (m, 1H).

Determination of K_i and k_{on} by a Competitive Method. To 1 mL solutions of 50 mM potassium phosphate, pH 7.2, and 100 μM NGD^+ containing 50, 25, 12.5, 6.25, and 0 μM inhibitor **1** was added 2 μL of 7 μM CD38. Reaction progress upon initiation by enzyme addition was monitored by measurement of 295 nm absorbance. The initial slopes were used to determine the K_i value, and all points of the experiment were fit to the equation:

$$A(t) = vt + (b - v)[1 - \exp(-kt)]/k + A_0$$

where k is the observed rate constant, b is the initial rate, v is the final rate, and A_0 is the initial absorbance used to evaluate k_{on}. A similar procedure was used for inhibitor **2**, with concentrations of components given in Figure 3.

Off-Rate Measurement. CD38 (500 nM) in 50 mM potassium phosphate, pH 7.2, was incubated with 15 μM inhibitor for 30 min at room temperature. Five microliters of the enzyme inhibitor solution was added to a cuvette containing 1 mL of 50 mM potassium phosphate, pH 7.5, containing 300 μM NGD^+ prechilled to 19 °C. Production of NGD^+ was determined by monitoring 295 nm absorbance. The absorbance was fit to the equation:

$$A(t) = vt + (b - v)[1 - \exp(-kt)]/k + A_0$$

where $A(t)$ is the absorbance, k is the rate constant of recovery, b is the initial rate, v is the final rate, and A_0 is the initial absorbance. A control lacking inhibitor but in all other respects identical was also run.

Radiochemical Measurement of Inhibitor Binding. [2′-^{3}H]-Nicotinamide deoxyriboside (**1**) was used to measure binding by the following method. Inhibitor at 9 μM with a specific radioactivity of 866 cpm/nmol was incubated with 1.2 μM CD38 (monomer) in 1 mL of 50 mM potassium phosphate (pH 7.5). The reactions were started by enzyme addition and quenched by freezing with a dry ice/acetone bath at 30, 60 90, 120, 250, 500, and 1000 s. Cooled (0 °C) gel filtration columns were used to separate protein using cooled (0 °C) 10 mM potassium phosphate as eluant. The frozen fraction was quickly thawed and applied to these columns, and fractions were collected in 1 mL volumes over the course of several minutes. Scintillation fluid (9 mL) was then added to each 1 mL fraction, and samples were counted. A sample lacking enzyme was used as a blank control as was a sample using the α-[2′-^{3}H]nicotinamide deoxyriboside of equal concentration and specific activity. The observed radioactivity was fit using the equation:

$$A(t) = A_0[1 - \exp(-kt)] + B$$

where A_0 is activity at reaction completion, k is the observed pseudo-first-order rate constant, and B is the activity of the blank.

Activity Recovery by Addition of Nicotinamide. CD38 (10 mL, 1 μM) in K_2HPO_4 was incubated with **2** (10 μM) for 30 min at room temperature and subsequently placed on ice. Ten 1.5 mL solutions of NGD^+ (400 μM) containing 0−100 mM nicotinamide were also prepared. To a two-syringe Applied Photophysics spectrophotometer in fluorescence mode were added inhibited enzyme to one syringe and NGD^+ solution to the other. Fluorescence was used to monitor cGDPR formation, and the total fluorescence curves were fit using the activity recovery equation:

$$F(t) = vt + (b - v)[1 - \exp(-kt)]/k + F_0$$

where k is the observed rate constant, b is the initial rate, v is the final rate, and F_0 is the initial absorbance. The value of k was plotted against the nicotinamide concentration, and the points were fit to the Michaelis−Menten equation using the program Kaleidagraph.

Base Exchange Reaction. Compound **2** (75 μM) was incubated with 1 μM CD38 enzyme and varying concentrations of nicotinamide (0−40 mM) in 150 μL volumes. These reactions were run separately in autosampler tubes held at 19 °C in a temperature-regulated autosampler and assayed by multi-injection HPLC using 5 mM K_2HPO_4, pH 5.0, and 2.5% MeOH as eluant. The quantity of **2** reacted and the quantity of **1** formed versus time were determined by integrations of the peaks for **1** and **2** with comparison to

Scheme 2: Synthetic Scheme for the Production of Pyridyl and Nicotinamide Deoxyriboside Inhibitors[a]

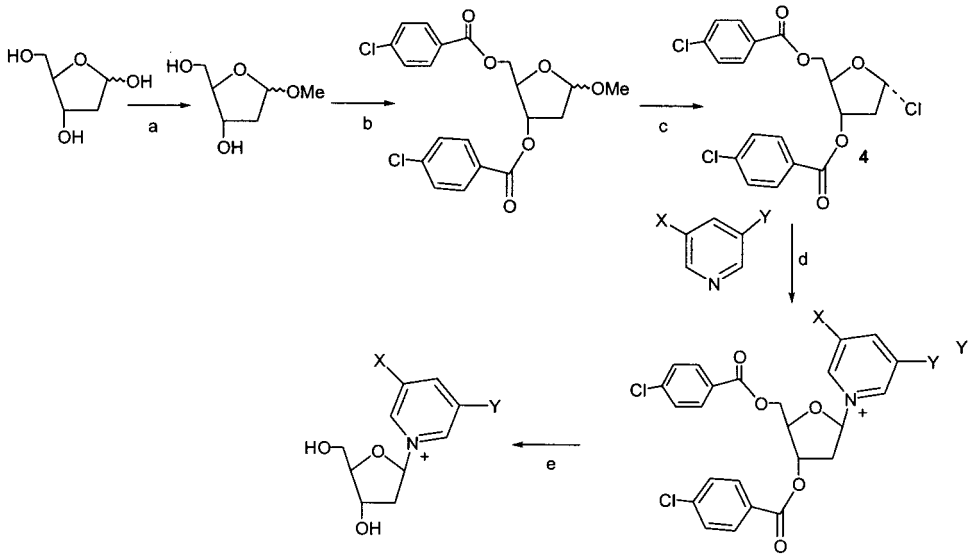

[a] Conditions: a, HCl, MeOH; b, *p*-chlorobenzoyl chloride, pyridine; c, AcOH, Et_2O, HCl, 273 K; d, 1.0 equiv of $AgSbF_6$, AcCN, 273 K; e, 2 M NH_3, MeOH.

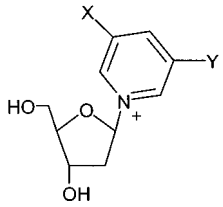

1: X= H, Y = $CONH_2$
2: X = Me, Y = $CONH_2$
3: X = H, Y = H

FIGURE 1: Structure of inhibitors **1**−**3**.

standards. The rate of conversion of **1** to **2** versus nicotinamide concentration was plotted, and the points were fit to the Michaelis−Menten equation using the program Kaleidagraph.

RESULTS

Synthesis of Nicotinamide 2′-Deoxyribosides. Several deoxynucleoside compounds (**1**−**3**, Figure 1) bearing 1′-β-pyridyl substitutions were prepared from the chloro sugar **4** (Scheme 2). In the sugar−base coupling step a stoichiometric quantity (versus sugar) of $AgSbF_6$ was found to significantly improve the stereochemical yield of the β isomer and the overall coupling yield. Standard deprotection protocol in cold methanolic ammonia gave the desired derivatives in mixtures of stereoisomers. Pure α and β stereoisomers were obtained by semipreparative reverse-phase HPLC.

Preparations of 2′-^{3}H-substituted versions of **1** and **2** were obtained by repeating the syntheses above with [2-^{3}H]-2-deoxyribose. This radiolabeled sugar starting material was obtained by digestion of commercially available [2′-^{3}H]-2′-deoxyuridine with the enzyme thymidine phosphorylase followed by treatment of the reaction mixture with alkaline phosphatase to form [2-^{3}H]deoxyribose (Scheme 3). The specific radioactivity of the inhibitors was determined to be 866 cpm/nmol.

Determination of Competitive Inhibition by Initial Rates. The inhibitors **1**−**3** were evaluated for inhibition of CD38 enzymatic activity using a spectrophotometric assay. CD38

Scheme 3: Synthetic Scheme To Obtain [2′-^{3}H]Deoxyribose from [2′-^{3}H]Deoxyuridine

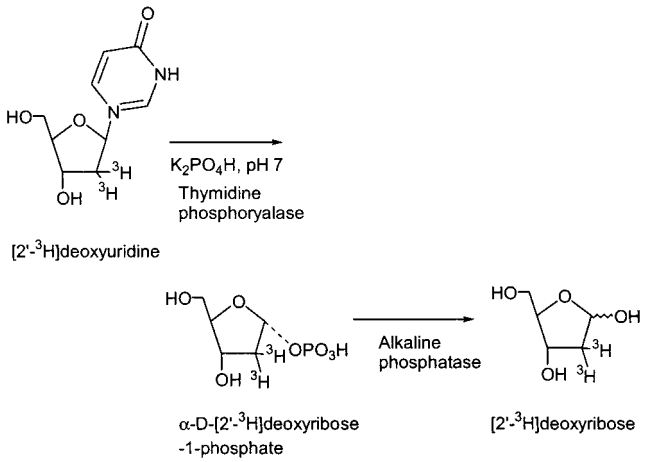

Scheme 4: NGD^+ Cyclization Reaction Catalyzed by ADP-ribosyl Cyclases

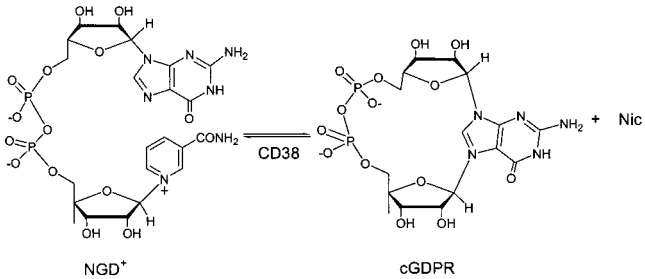

catalyzes the conversion of NGD^+ to cyclic GDP-ribose (cGDPR, Scheme 4), and product formation can be monitored by 295 nm absorbance measurement. Figure 2 shows the behavior of **1** in assays using 100 μM NGD^+ (50×K_m, *35*) and variable inhibitor concentrations. The initial rates of these reactions (Figure 2A) demonstrated competitive inhibition of CD38 cyclase activity by **1** with a value for K_i of 1.2 μM ± 0.3. A similar reaction containing 40 μM NGD^+ at several concentrations of **2** was also performed (Figure 3). Initial rates of reaction showed inhibition of CD38 cyclase

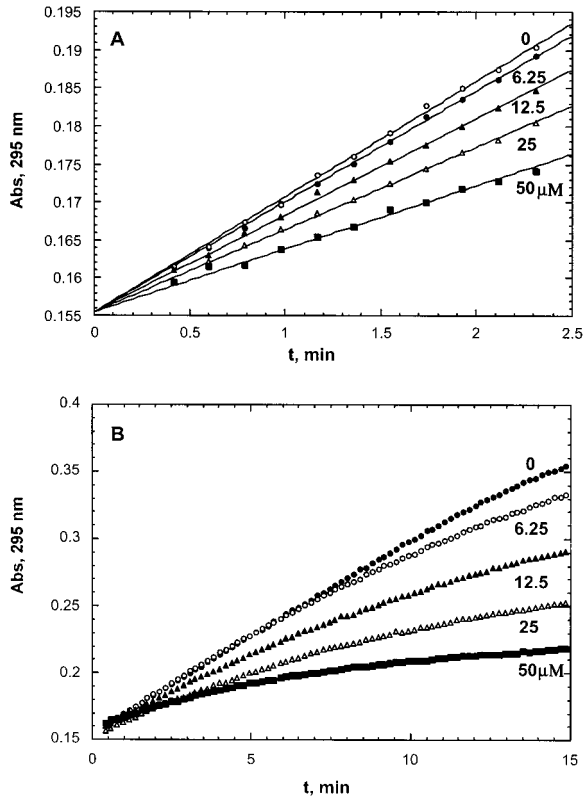

FIGURE 2: Time courses of inhibition of CD38 by different concentrations of **1** as assayed by conversion of NGD^+ to cGDPR (100 μM NGD^+). (A) Initial rates of reaction of curves from panel B were fit to the equation for competitive inhibition to determine K_i in Table 1. (B) Extended time courses of two-phase inhibition of CD38 by different concentrations of **1** as assayed by conversion of NGD^+ to cGDPR. Inhibitor concentrations are shown. The solid lines represent the best fit to the slow-onset equation given in the text. The rate constant (k_1) for the slow phase derived from these curves is 4.2×10^{-3} s^{-1}.

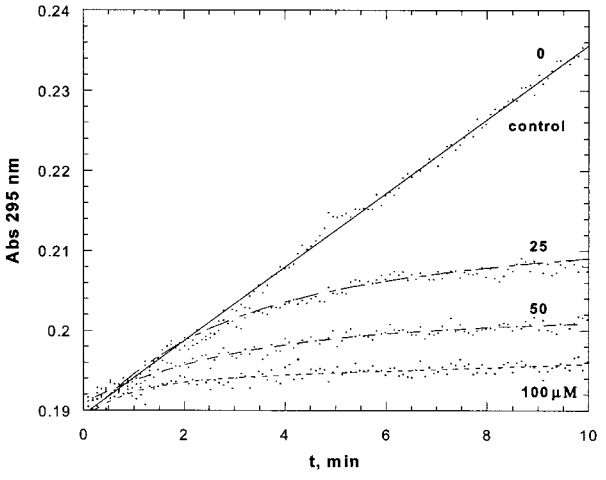

FIGURE 3: Time course of two-phase inhibition of CD38 by different concentrations of **1** as assayed by conversion of NGD^+ to cGDPR (40 μM NGD^+). Inhibitor concentrations are shown on the right of the curves. The solid lines represent the best fit to the slow-onset equation given in the text. The rate constant (k_{on}) for the slow phase derived from these curves is 8.3×10^{-3} s^{-1}. The initial rates from these curves were used to determine K_i (Table 1).

activity by **2** with a K_i of 4.0 $\pm$ 0.5 μM. Reaction mixtures containing **3**, the α isomer of **1**, or the α isomer of **2** did not inhibit CD38 conversion of NGD^+ to cGDPR even at millimolar concentrations of these compounds (data not shown).

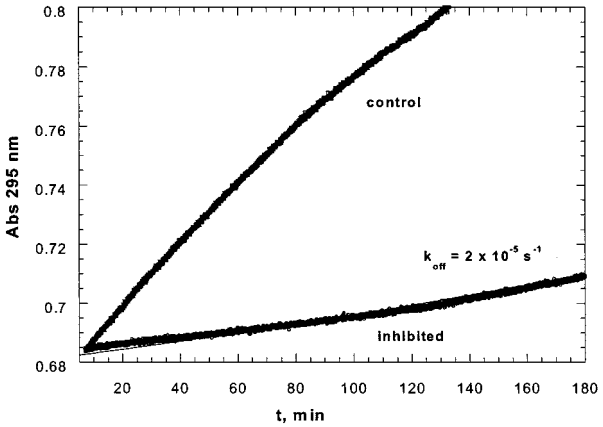

FIGURE 4: Recovery experiment to measure the rate of recovery of CD38 from inhibition by **1** in the presence of excess NGD^+. The top curve is a control: uninhibited enzyme. The bottom curve shows the recovery process as increasing free CD38 generates increasing rates of cGDPR formation. The solid curve represents the best fit to the recovery equation described in the text. The recovery rate determined was 2×10^{-5} s^{-1}.

Scheme 5: Theoretical Scheme To Characterize Two-Phase Inhibition

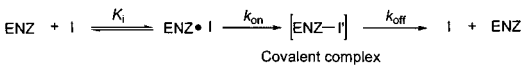

Slow-Phase Inhibition. Reaction progress curves of CD38 activity in reaction mixtures containing the inhibitors **1** and **2** showed not only initial rate inhibition but a second phase of slow-onset inhibition indicated by slopes declining monotonically over time as seen in Figures 2 and 3. This slow phase was not due to substrate depletion and was attributable to a kinetic process leading to progressive inhibition of the enzyme. The "slow-onset" absorbance curves could be fit using the equation:

$$A_t = v_i t + (v_i - v_f)[1 - \exp(-kt)]/k + A_0$$

where A_t is absorbance, v_i is initial velocity, v_f is final velocity, t is time in seconds, k is the rate of the slow-onset process, and A_0 is absorbance of the sample at initial time. These fits are shown by the solid lines in Figures 2 and 3. The rate constant for the slow phase could be obtained from the average value of k determined from the separate fits. The value of k for **1** was determined to be 0.0042 $\pm$ 0.001 s^{-1}, and the value of k for **2** was determined to be 0.0083 $\pm$ 0.002 s^{-1}. The parameter k is defined as k_{on} in Scheme 5.

Recovery from Inhibition. To fully characterize the inhibition of **1** and **2** against CD38, determinations of the inhibitor off-rates were needed. The inhibitor off-rate provides the final parameter in the equation $(k_{off}/k_{on})K_i = K_{i(total)}$, which is valid for the kinetic scheme of slow-onset inhibition shown in Scheme 5. This rate was obtained by a recovery protocol in which inhibited CD38 enzyme (by either **1** or **2)** was added to a 200 μM solution of NGD^+. The solution 295 nm absorbance is monitored spectrophotometrically to assay conversion of NGD^+ to cGDPR as a consequence of regain of CD38 catlytic activity. Typical curves obtained are shown in Figure 4. The top curve shows product formation of a control reaction using uninhibited CD38, and the bottom

Table 1: Kinetic and Equilibrium Parameters for Inhibitors **1** and **2**[a]

parameter	**1**	**2**
K_i (μM)	1.2	4.0
k_{on} (s^{-1})	4.2×10^{-3}	8.3×10^{-3}
k_{off} (s^{-1})	1.5×10^{-5}	2.5×10^{-5}
$K_{i(total)}$ (nM)	4.5	12.5

[a] All values obtained at 19 °C. The parameters are defined in accord with Scheme 5. The value for $K_{i(total)}$ was obtained by the relation $K_{i(total)} = (k_{off}/k_{on})K_i$. The values for each parameter in the calculation is given in the table.

curve shows slow recovery of activity of inhibited enzyme versus time. The absorbance curves with the same equation were used for slow onset:

$$A_t = v_i t + (v_i - v_f)(1 - \exp(-kt))/k + A_0$$

where A_t is absorbance, v_i is initial velocity, v_f is final velocity, t is time in seconds, k is the rate of the recovery rate constant, and A_0 is the absorbance of the sample at initial time. The rate constant for the recovery phase was obtained from the average value of k determined from the separate fits. The value of k_{off} for **1** was determined to be 1.5×10^{-5} s^{-1} and for **2** was determined to be 2.5×10^{-5} s^{-1}.

Calculation of Total Inhibition. Inhibition of CD38 by compounds **1** and **2** could be fully described by the equation $(k_{off}/k_{on})K_i = K_{i(total)}$ for the reactions described by Scheme 5, where $K_{i(total)}$ is the effective dissociation constant between free CD38 and the fully inhibited complex. This equation is valid for slow-onset behavior inhibitors and also for mechanistic-based inactivators of enzymes where a slow recovery of the enzyme from chemical inactivation is present. Using the kinetic parameters in Table 1 the value for $K_{i(total)}$ is 4.5 nM for inhibitor **1**. Similarly, a value for $K_{i(total)}$ of 12.5 nM was calculated for inhibitor **2**.

Nature of Inhibition in the Slow Phase: Rescue by Base Addition. Our prior investigations of the nature of inhibition of CD38 by *ara*-F-NMN^+ showed it to be governed by both competitive and slow-onset characteristics (*23*). The slow-onset behavior was shown to be a consequence of covalent trapping of the catalytic nucleophile (Glu226) by the *ara*-F sugar with nicotinamide leaving group departure. By analogy, the slow-onset inhibition of deoxynucleosides **1** and **2** is proposed to proceed via deoxyribose sugar transfer to the catalytic nucleophile. To test this hypothesis, additional chemical methods were used to examine the scheme of inactivation shown in Scheme 6.

According to Scheme 6 recovery of enzymatic activity occurs via slow hydrolysis of the covalent intermediate to form deoxyribose and free enzyme. If the covalent intermediate is the normal catalytic reaction path, the enzyme catalytic activity should also be recovered from inhibition by reaction with a substrate nucleophile, such as nicotinamide (Scheme 7). The rate and equilibrium of the reaction will establish the thermodynamic equilibrium of these species. For favorable equilibria, addition of product pyridine bases should permit base exchange reactions that will rapidly regenerate active enzyme. Rescue of activity by substrate nucleophiles has been used as a test of the covalent mechanism in the *ara*-F-NMN^+ inactivation of CD38, with rescue by nicotinamide (*23*), and has been observed in the

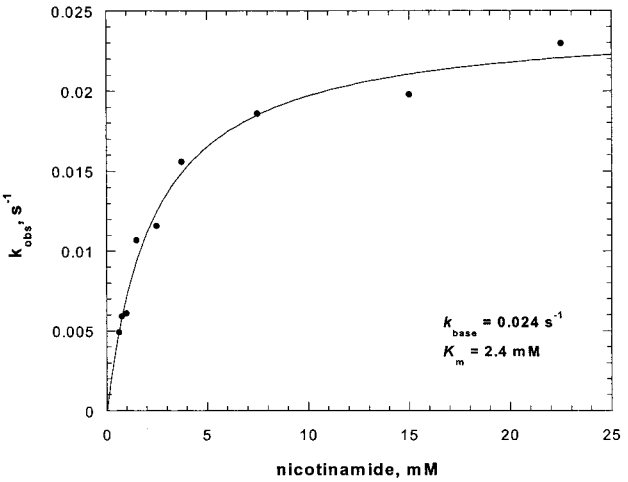

FIGURE 5: Rates of CD38 recovery as a function of nicotinamide concentration as determined by stopped flow. The apparent Michaelis parameters were derived from the best fit of the points to the Michaelis−Menten equation. The parameter k_{base} is defined in Scheme 7.

Scheme 6: Mechanistic Scheme of CD38 Inhibition by Nicotinamide- and 5-Methylnicotinamide-Substituted Deoxyribose Derivatives

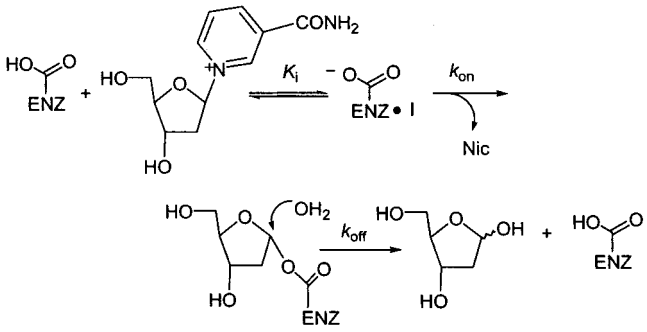

covalent inactivation of nucleoside 2′-deoxyribosyltransferase (*36*) and other covalently inactivated glycosyl transferases (*37*).

The rescue experiment involved preincubation of CD38 with the inhibitor **2** followed by reaction of enzyme with a 300 μM solution of NGD^+ containing different concentrations of nicotinamide as a regenerating base. A stopped-flow, two-syringe fitted spectrophotometer was used to perform the experiments. The fluorescence of cGDPR was measured as a function of time to generate curves that contain an exponential and a linear phase prior to substrate exhaustion. These curves were fit to the equation

$$F_t = v_f t + (v_i - v_f)[1 - \exp(-kt)]/k + F_0$$

as previously defined. The rate constant k_{base} was plotted against the nicotinamide concentration to obtain a saturation curve with an apparent apparent K_m value for nicotinamide of 2.4 mM and a maximum rate of 0.023 s^{-1} (Figure 5). The limiting value of k_{base} as nicotinamide concentration is increased indicates equilibrium binding of nicotinamide at the active site prior to chemical reaction. Therefore, the K_m represents an accurate measurement of K_d for nicotinamide for the covalent form of the enzyme. Similar saturation curves have been reported for the rescue behavior of adenine on 2′-fluoroadenosine inactivation of nucleoside 2′-deoxyribosyltransferase (*36*) and for nicotinamide rescue of CD38 from *ara*-F-NMN^+ inactivation (*23*).

Scheme 7: Mechanistic Scheme of CD38 Inhibition by **2** and Rescue by Nicotinamide To Form **1**

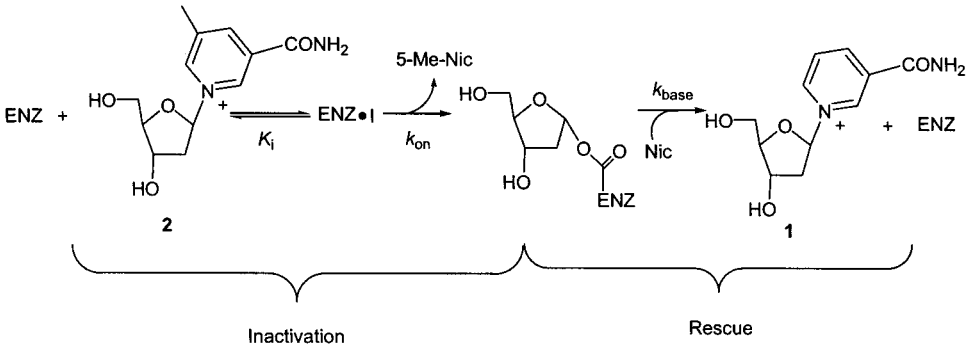

Base Exchange Reaction. The nicotinamide rescue of CD38 enzymatic activity inhibited by **2** completes a catalytic cycle that is proposed to effect base exchange of **2** to form **1**. The rescue reaction is the second half of the normal reaction cycle of the base exchange reaction catalyzed by CD38, and inactivation of CD38 by **2** is the first half. This hypothesis was tested by incubation of 75 μM **2** with varying concentrations of nicotinamide in the presence of 1 μM CD38, and the reactions were monitored by HPLC. Figure 6 shows that CD38 catalyzes the conversion of **2** to **1** under these conditions. The peak at 8 min elutes identically with authentic **1**. The rates of these reactions could be monitored by multiple autosampler-driven injections and the rates of conversion plotted against nicotinamide concentration. The points were fit using the Michaelis−Menten equation (Figure 7) to obtain a K_m of 0.92 mM for nicotinamide and a k_{cat} of 0.007 s^{-1}. The observed k_{cat} value is within experimental error of the rate of inactivation (k_{on} = 0.008 s^{-1}, Scheme 5) of CD38 by **2** measured at the same temperature. This result establishes that the rate of intermediate formation is rate limiting in the catalytic cycle of Scheme 7. The greater than 2-fold lower K_m for steady-state base exchange (0.92 mM) versus the apparent K_m for nicotinamide rescue (2.4 mM) suggests that submaximal base binding to the nicotinamide binding pocket during steady-state conditions is sufficient to maintain the maximum turnover rate. This notion is supported by the rate constant for formation of the covalent intermediate (k_{on} = 0.008 s^{-1}) and the rate constant for the base reaction step (k_{base} = 0.023 s^{-1}) measured independently.

Titration of Enzyme with 2′-^{3}H-Substituted Inhibitor. CD38 inactivation was accomplished using a radiolabeled inhibitor to assess inhibitor interactions with the enzyme independent from inhibition of the catalytic activity. This method allows the determination of the stoichiometry of covalent labeling and detects cooperativity at multiple sites. The labeling characteristics of CD38 show that it is labeled by **1** in a process governed by a single rate constant with a value of k_{chem} = 0.01 s^{-1} at 25 °C (Figure 8), within reasonable agreement with the rate constant for inactivation in kinetic

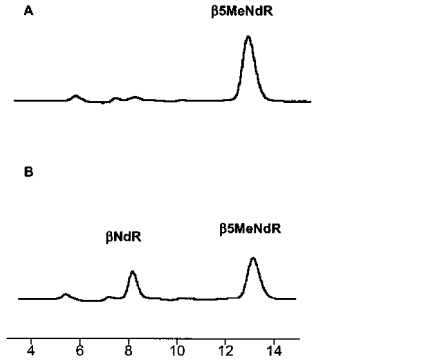

FIGURE 6: HPLC chromatograms of base exchange reaction solutions. (A) Initial chromatogram at 0 time containing 1 μM CD38, 75 μM **2**, and 20 mM nicotinamide. (B) Chromatogram of the same solution after several hours of incubation at 19 °C showing the appearance of the base-exchanged product β-nicotinamide 2′-deoxyriboside (**1**). Abbreviations: β5MeNdR, β-5-methylnicotinamide 2′-deoxyriboside; βNdR, β-nicotinamide 2′-deoxyriboside.

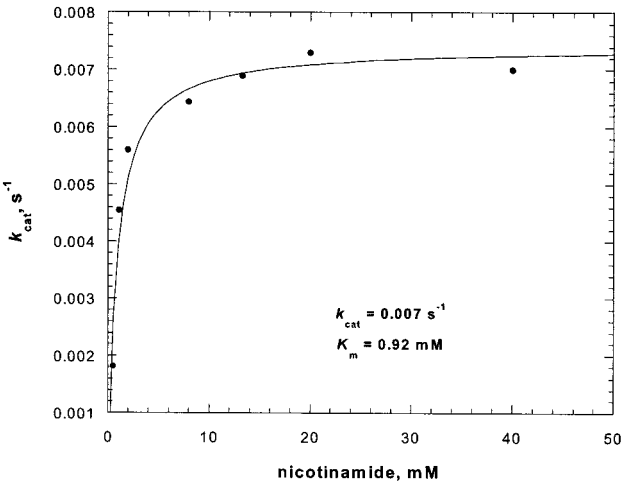

FIGURE 7: Steady-state rate of base exchange of CD38 in which **2** forms **1** by reaction with nicotinamide. The Michaelis parameters were derived from the best fit of the points to the Michaelis−Menten equation.

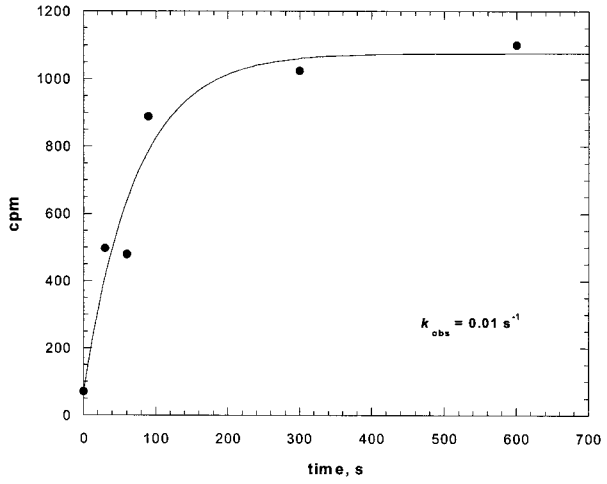

FIGURE 8: Radiochemical labeling of 1 nmol of CD38 (monomer) by [2-^{3}H]-**1** as measured by gel filtration and scintillation counting. The solid curve represents the best fit to the equation $P = A + A_2 \exp(-kt)$. The curve obtains a value of k of 0.01 s^{-1}. The specific radioactivity of the inhibitor is 866 cpm/nmol.

assays of inhibition (k_{on} = 0.0042 s^{-1} at 19 °C). The extent of labeling does not change after the first 20 min of incubation time, which indicates that there is no nonspecific labeling of the enzyme by the inhibitor. According to specific activity measurements and protein concentration, the labeling is 1:1 versus CD38 monomer concentration. This result is similar to what was observed with CD38 inhibition by *ara*-F-NMN^+ (*23*).

DISCUSSION

Nicotinamide deoxyriboside derivatives bind to the catalytic sites of CD38 with higher binding affinity than the natural substrate, NAD^+. **1** has a binding constant of 1.2 μM and **2** has a binding constant of 4 μM. In comparison, the K_m for dinucleotide and mononucleotide substrates is 150 μM for NMN^+ (*35*), 15 μM for NAD^+, and 2.5 μM for NGD^+. On the basis of these comparisons, it is apparent that truncation of structure does not necessarily weaken binding. Inhibition of CD38 by the deoxynucleoside compounds **1** and **2** not only is competitive but is characterized by a second kinetic phase of inhibition marked by enhanced affinity of the inhibitor for the enzyme with rates of onset of 0.004 s^{-1} for **1** and 0.008 s^{-1} for **2**. Recovery of the enzyme from the second phase of binding is quite slow, on the order of 2×10^{-5} s^{-1} at 19 °C, and was similar within experimental error for both **1** and **2**. By use of the equation for slow-onset inhibitors, $K_i(k_{off}/k_{on}) = K_{i(total)}$, the enhanced binding leads to inhibition values of 4.5 nM for inhibition of CD38 by **1** and 12.5 nM by **2**. These inhibition constants are lower than any known CD38 inhibitors and confirm that highly abbreviated structures can rapidly and potently inhibit ADP-ribosyl cyclase enzymes. The magnitude of the rate constants for inactivation (k_{on}) shows that tight inhibition can be achieved within minutes at physiological temperatures.

The nature of the slow-phase process leading to formation of the tight complex in Scheme 5 is proposed to be the covalent modification of the enzyme by inhibitor via attachment of the deoxyribose sugar to the enzyme catalytic nucleophile as shown in Scheme 6. A previous example of covalent modification of CD38 revealed that the inhibitor *ara*-F-NMN^+ forms a stable *ara*-F-ribose 5-phosphate ester with Glu226 (*23*). MS studies confirmed the identity of this acid as the catalytic nucleophile. This residue is universally conserved across all ADP-ribosyl cyclase sequences and has been mutagenized with ablation of catalytic activity for CD38 (*38*). The covalent modification was shown to be reversible, and nicotinamide additions to the trapped enzyme recover catalytic activity and re-form *ara*-F-NMN^+. Moreover, CD38 catalyzes base exchange using *ara*-F-NMN^+ as a substrate.

Similar behaviors were observed for inhibited CD38 treated with the deoxy inhibitors **1** and **2**. For instance, when fully inhibited CD38 enzyme (by either **1** or **2**) was treated with millimolar concentrations of nicotinamide, recovery of catalytic activity was observed, with a rate of recovery dependent on nicotinamide concentration. The recovery rate reached a saturable maximum versus nicotinamide concentration. Rate saturation for recovery has also been observed in previous studies of covalent intermediates, and the apparent K_m appears to reflect the binding affinity of the rescue nucleophile within the active site. This value was found to be 17 mM for *ara*-F-NMN^+ rescue by nicotinamide (*23*), and the 2.4 mM value for rescue from the deoxyribose intermediate indicates that nicotinamide binding is tighter in the covalent complex formed by deoxyribose modification of CD38.

Scheme 7 shows inactivation and recovery as two mechanistic steps in a catalytic cycle that leads to inhibitor base exchange. Incubations of **2** with nicotinamide confirmed that CD38 catalyzes base exchange to form **1** and 5-methylnicotinamide. HPLC analysis was used to monitor the kinetics of base exchange because **1** is readily separated from **2** and base exchange is fairly slow. The K_m of nicotinamide for base exchange is 0.92 mM, and the k_{cat} is 0.007 s^{-1} at 19 °C. The value of K_m for base exchange (0.92 mM) is significantly lower than the value for the apparent K_m for base rescue (2.4 mM) of CD38 activity from inhibition by **2**. However, the rate of rescue saturates at 0.024 s^{-1}, suggesting that the lower K_m for exchange takes its origin from the chemistry of covalent modification of the enzyme being rate limiting in the catalytic cycle and because full-site binding by base is unnecessary to maintain the steady-state rate in the second reaction of base exchange. Thus, the rate of turnover of base exchange matches the rate of slow-phase inhibitor inactivation by **2**, which has the value 0.008 s^{-1}.

Radiochemical titrations of enzyme with [2′-^{3}H]-**1** confirm that labeling reaches a maximum with a rate constant of 0.01 s^{-1} and extended incubations do not increase radiochemical labeling. The extent of labeling is consistent with a ratio of inhibitor to subunit of 1:1. These measurements confirm that covalent modification is a specific process and is due to the covalent modification of the catalytic nucleophile responsible for catalysis with faster substrates.

The effectiveness of deoxynucleosides as trapping agents for CD38 is in contrast to chemical stability profiles. 2′-Deoxy derivatives are intrinsically more labile to uncatalyzed solvolysis reactions than the corresponding ribose derivatives and even more unstable than 2′-fluorine-substituted derivatives (*39*). Trapping of covalent intermediates on nucleoside and glycosyl transferase enzymes has been successful in a number of cases by the introduction of 2′-fluorine (*23*, *36*, *37*),because of the electronic destabilization of the cationic charge that builds up at the anomeric carbon in transition states common to nucleoside and glycosyl transfer reactions. The increase in energy of these transition states retards breakdown of trapped intermediates (*37*). In examination of the rate of turnover of NMN^+ versus *ara*-F-NMN^+ on CD38 it was intriguing to note that the ratio of the rates of turnover of CD38 covalent intermediates was on the order of 10^7 at 37 °C (*23*, *35*), which did not match the ratio of their uncatalyzed solvolysis rates, which was measured to be 30:1 at the same temperature (*39*). This suggested that slow turnover of fluorine-substituted intermediates by CD38 took most of its origin from removal of the 2′-OH group and not from an electronic effect contributed by fluorine.

The results of this study strongly corroborate this viewpoint. In this case removal of the 2′-OH and replacement with a hydrogen atom in conjunction with removal of the 5′-phosphate group lead to efficient formation of the covalent intermediate but inefficient hydrolytic turnover of this species, leading to effective trapping and inhibition of the enzyme. The role of the 2′-OH in catalysis is suggested by the proximity it normally has to the Glu226 leaving group

which departs the sugar in intermediate breakdown. Both share the α face of the sugar, and proton transfer to the Glu residue during catalytic turnover may be mediated in part by the 2′-OH. The proposed protonation state of the catalytic Glu during catalysis is indicated in Scheme 6. Although this rationale deserves additional investigation, a strong Glu−2′-OH interaction has been proposed as a part of NAD^+ glycohydrolase function (*39*) and has recently been revealed crystallographically in the enzyme BST-1 (*40*).

Trapping efficiency can also improve from the lack of the ADP group in inhibitors **1** and **2**. The nucleoside structure lacks the adenylate of the normal NAD^+ substrate, thus precluding the normal cyclization pathway inherent to dinucleotide substrates. The absence of a reasonable nucleophile for an escape from the intermediate complex via the intramolecular route leaves hydrolysis as the only remaining escape pathway.

In conclusion, deoxynucleosides are effective mechanism-based inhibitors of CD38 through formation of a covalent intermediate that has been identified as part of the normal reaction coordinate of CD38 catalysis. A variety of techniques establish that this inactivation is specific to a single reactive moiety on the enzyme, which is catalytically competent to support the base exchange mechanism inherent to CD38 catalysis with faster substrates. These compounds lack phosphate groups, have nanomolar binding affinity for CD38 enzymes, inactivate within minutes at room temperature, and have slow recovery rates, suggesting that these derivatives may be effective probes of CD38 biochemical action in cells and tissues.

ACKNOWLEDGMENT

The authors thank Dr. Hon-Cheung Lee for a gift of the yeast strain expressing the soluble human CD38 used in this study. In addition, we thank Dr. HaiTeng Deng, who performed MS characterization of **1**.

REFERENCES

1. Jackson, D. G., and Bell, J. I. (1990) *J. Immunol. 144*, 2811−2815.
2. Fernandez, J. E., Deaglio, S., Donati, D., Saoboda Beusan, I., and Corno, F. (1998) *J. Biol. Regul. Homeostatic Agents 12*, 81−91.
3. Kato, I., Takasawa, S., Akabane, A., Tanaka, O., and Abe, H. (1995) *J. Biol. Chem. 270*, 30045−30050.
4. Khoo, K. M., and Chang, C. F. (2000) *Arch. Biochem. Biophys. 373*, 35−43.
5. Mizuguchi, M., Otsuka, N., Sato, M., Ishii, Y., and Kon, S. (1995) *Brain Res. 697*, 235−240.
6. Kaisho, T., Ishikawa, J., Oritani, K., Inazawa, J., Tomizawa, H., and Muroaka, O. (1994) *Proc. Natl. Acad. Sci. U.S.A. 91*, 5325−5329.
7. Itoh, M., Ishihara, K., Tomzawa, H., Tanaka, H., Kobune, Y., and Ishikawa, J. (1994) *Biochem. Biophys. Res. Commun. 203*, 1309−1317.
8. Lee, H. C., and Aarhus, R. (1991) *Cell Regul. 2*, 203−209.
9. States, D. J., Walseth, T. F., and Lee, H. C. (1992) *Trends Biochem. Sci. 17*, 495.
10. Lee, H. C., Aarhus, R., and Levitt, D. (1994) *Nat. Struct. Biol. 1*, 143−144.
11. Rusinko, N., and Lee, H. C. (1989) *J. Biol. Chem. 264*, 11725−11731.
12. Howard, M., Grimaldi, J. C., Bazan, J. F., Lund, F. E., and Santos-Argumedo, L. (1993) *Science 262*, 1056−1059.
13. Lee, H. C. (2001) *Annu. Rev. Pharmacol. Toxicol. 41*, 317−345.
14. Lee, H. C. (1996) *Recent Prog. Horm. Res. 51*, 355−388.
15. Clapper, D. L., Walseth, T. F., Dargie, P. J., and Lee, H. C. (1987) *J. Biol. Chem. 262*, 9561−9568.
16. Partida-Sanchez, S., Cockayne, D. A., Monard, S., Jacobson, E. L., Oppenheimer, N., Garvy, B., Kusserm K., Goodrich, S., Howard, M., Harmsen, A., Randall, T. D., and Lund, F. E. (2001) *Nat. Med. 11*, 1209−1216.
17. Normark, S., Normark, B. H., and Hornet, M. (2001) *Nat. Med. 11*, 1182−1184.
18. Wu, Y., Kuzma, J., Marechal, E., Graeff, R., and Lee, H. C. (1997) *Science 278*, 2126−2130.
19. Sleath, P. R., Handlon, A. L., and Oppenheimer, N. J. (1991) *J. Org. Chem. 56*, 3608−3613.
20. Muller-Steffner, H. M., Malver, O., Hosie, L., Oppenheimer, N. J., and Schuber, F. (1992) *J. Biol. Chem. 267*, 9606−9611.
21. Bethelier, V., Tixier, J. M., Muller-Steffner, H., Schuber, F., and Deterre, P. (1998) *Biochem. J. 330*, 1383−1390.
22. Wall, K. A., Klis, M., Kornet, J., Coyle, D., Ame, J. C., Jacobson, M. K., and Slama, J. T. (1998) *Biochem. J. 335*, 631−636.
23. Sauve, A. A., Deng, H. T., Angeletti, R. H., and Schramm, V. L. (2000) *J. Am. Chem. Soc. 122*, 7855−7859.
24. Sato, A., Yamamoto, S., Kajimura, N., Oda, M., Usukura, J., and Jingami, H. (1999) *Eur. J. Biochem. 264*, 439−445.
25. Sato, A., Yamamoto, S., Ishihara, K., Hirano, T., J., and Jingami, H. (1999) *Biochem. J. 337*, 491−496.
26. Hara-Yokoyama, M., Nagatsuka, Y., Katsumata, O., Irie, F., Kontani, K., Hoshino, S., Katada, T., Ono, Y., Fujita-Yoshhigaki, J., Sugiya, H., Furuyama, S., and Hirabayashi, Y. (2001) *Biochemistry 40*, 888−895.
27. Walseth, T. F., and Lee, H. C. (1993) *Biochim. Biophys. Acta 1178*, 235−242.
28. Sethi, J. K., Empson, R. M., Bailey, V. C., Potter, B. V. L., and Galione, A. (1997) *J. Biol. Chem. 272*, 16358−16363.
29. Walseth, T. F., Aarhus, R., Kerr, J. A., and Lee, H. C. (1993) *J. Biol. Chem. 268*, 26686−26691.
30. Ashamu, G. A., Sethi, J. K., Galione, A., and Potter, B. V. L. (1997) *Biochemistry 36*, 9509−9517.
31. Galione, A., Lee, H. C., and Busa, W. B. (1997) *Science 253*, 1143−1146.
32. Wong, L., Aarhus R., Lee H. C., and Walseth, T. F. (1999) *Biochim. Biophys. Acta 1472*, 555−564.
33. Lee, H. C., and Aarhus, R.(1998) *Biochim. Biophys. Acta 1425*, 263−271.
34. Bailey, V. C., Fortt, S. M., Summerhill, R. J., Galione, A., and Potter, B. V. L. (1996) *FEBS Lett. 379*, 227−228.
35. Sauve, A. A., Munshi, C., Lee, H. C., and Schramm, V. L. (1998) *Biochemistry 37*, 13239−13249.
36. Porter, D. J., Merrill, B. M., and Short, S. A. (1995) *J. Biol. Chem. 270*, 15551−15556.
37. Withers, S. G. (2000) *Acc. Chem. Res. 33*, 11−18.
38. Munshi, C., Theil, D., Mathews, I. J., Aarhus, R., Walseth, T. F, and Lee, H. C. (1999) *J. Biol. Chem. 274*, 30770−30777.
39. Oppenhemer, N. J., and Handlon, A. L. (1992) in *The Enzymes* (Sigman, D. L., Ed.) Vol. 20, Chapter 10, pp 453−505, Academic Press, San Diego, CA.
40. Yamamoto-Katayama, S., Ariyoshi, M., Ishihara, K., Hirano, T., Jingami, H., and Morikawa, K. (2002) *J. Mol. Biol. 316*, 711−723.
41. Fox, J. J., Yung, N. C., Wempen, I., and Hoffer, M. (1961) *J. Am. Chem. Soc. 83*, 4066−4072.
42. Handlon, A. L., and Oppenheimer, N. J. (1991) *J. Org. Chem. 56*, 5009−5010.

BI0258795